Intersectin associates with synapsin and regulates its nanoscale localization and function

Fabian Gerth[a,1], Maria Jäpel[b,1], Arndt Pechstein[a,b,1], Gaga Kochlamazashvili[b], Martin Lehmann[b], Dmytro Puchkov[b], Franco Onofri[c], Fabio Benfenati[c,d], Alexander G. Nikonenko[e], Kristin Fredrich[f], Oleg Shupliakov[f,g], Tanja Maritzen[b], Christian Freund[a,2], and Volker Haucke[a,b,2]

[a]Faculty of Biology, Chemistry, and Pharmacy, Freie Universität Berlin, 14195 Berlin, Germany; [b]Department of Molecular Pharmacology and Cell Biology, Leibniz-Forschungsinstitut für Molekulare Pharmakologie, 13125 Berlin, Germany; [c]Department of Experimental Medicine, University of Genoa, 16132 Genoa, Italy; [d]Center for Synaptic Neuroscience and Technology, Istituto Italiano di Tecnologia, 16163 Genoa, Italy; [e]Department of Cytology, Bogomoletz Institute of Physiology, 01024 Kiev, Ukraine; [f]Department of Neuroscience, Karolinska Institutet, 171 77 Stockholm, Sweden; and [g]Institute of Translational Biomedicine, St. Petersburg State University, 199034 St. Petersburg, Russia

Edited by Pietro De Camilli, Howard Hughes Medical Institute, Yale University, New Haven, CT, and approved September 28, 2017 (received for review September 1, 2017)

Neurotransmission is mediated by the exocytic release of neurotransmitters from readily releasable synaptic vesicles (SVs) at the active zone. To sustain neurotransmission during periods of elevated activity, release-ready vesicles need to be replenished from the reserve pool of SVs. The SV-associated synapsins are crucial for maintaining this reserve pool and regulate the mobilization of reserve pool SVs. How replenishment of release-ready SVs from the reserve pool is regulated and which other factors cooperate with synapsins in this process is unknown. Here we identify the endocytic multidomain scaffold protein intersectin as an important regulator of SV replenishment at hippocampal synapses. We found that intersectin directly associates with synapsin I through its Src-homology 3 A domain, and this association is regulated by an intramolecular switch within intersectin 1. Deletion of intersectin 1/2 in mice alters the presynaptic nanoscale distribution of synapsin I and causes defects in sustained neurotransmission due to defective SV replenishment. These phenotypes were rescued by wild-type intersectin 1 but not by a locked mutant of intersectin 1. Our data reveal intersectin as an autoinhibited scaffold that serves as a molecular linker between the synapsin-dependent reserve pool and the presynaptic endocytosis machinery.

neurotransmission | synaptic vesicles | multidomain scaffold | intramolecular regulation | NMR spectroscopy

Neurotransmission is based on the fusion of readily releasable synaptic vesicles (SVs) at the presynaptic active zone (1, 2). Fusing SVs are concomitantly replenished by compensatory endocytosis of SV membranes and clathrin-mediated reformation of SVs (3, 4). During sustained periods of activity the recycling vesicle pool is refilled by mobilization of SVs from the reserve pool (5). The synapsins (synapsin I, II, and III), are major SV-associated phosphoproteins encoded by three distinct genes that are required for the formation and maintenance of the reserve/recycling pools of SVs via association with the actin cytoskeleton (6–8). Activity-dependent phosphorylation of synapsin I by several kinases at distinct sites regulates its association with SV membranes and F-actin to control SV mobilization from the reserve pool (6). Consistently, loss of synapsin I causes depletion of reserve pool SVs and a marked impairment in inhibitory transmission (9, 10), resulting in an epileptic and autistic phenotype in mice (8, 11) and humans (12).

Endocytic proteins are enriched within the presynaptic compartment at steady state (13). Upon synaptic activity they are recruited to the so-called "periactive zone" that surrounds active zone (AZ) release sites to facilitate endocytic membrane internalization and SV reformation. Among the endocytic proteins shown to undergo activity-dependent movement to the periactive zone are intersectin 1 and 2, large scaffolds containing five Src homology domain 3 (SH3) domains (Fig. S1*A*), which bind to a plethora of exo/endocytic and actin regulatory proteins. Intersectins have been suggested to regulate actin dynamics and to couple the exo/endocytic limbs of the SV cycle (14). Intersectin 1 deletion in mice causes a comparably mild presynaptic phenotype (15, 16), while its overexpression is associated with Down syndrome in humans (17). Loss of Dap160, the *Drosophila melanogaster* homolog of mammalian intersectins, has been linked to defects in neurotransmission, SV cycling, and SV pool organization (18, 19), suggesting that intersectins serve as multifunctional scaffolds that coordinate different steps in the SV cycle (14). How these diverse functions of intersectin are controlled in molecular terms is unknown.

Here we combine mouse genetics, superresolution imaging, electrophysiology, and NMR-based structural studies to identify a key role for intersectin in SV replenishment at hippocampal synapses by regulated complex formation with synapsin I.

Results

Intersectin Associates with Synapsin I in Central Synapses. The molecular basis for the enrichment of endocytic proteins in nerve terminals (13) is unknown. Hence, we screened for possible interactions between known presynaptic components and the endocytic

Significance

Mutations in genes regulating neurotransmission in the brain are implicated in neurological disorders and neurodegeneration. Synapsin is a crucial regulator of neurotransmission and allows synapses to maintain a large reserve pool of synaptic vesicles. Human mutations in synapsin genes are linked to epilepsy and autism. How synapsin function is regulated to allow replenishment of synaptic vesicles and sustain neurotransmission is largely unknown. Here we identify a function for the endocytic scaffold protein intersectin, a protein overexpressed in patients with Down syndrome, as a regulator of synapsin nanoscale distribution and function that is controlled by a phosphorylation-dependent autoinhibitory switch. Our results unravel a hitherto unknown molecular connection between the machineries for synaptic vesicle reserve pool organization and endocytosis.

Author contributions: A.P., G.K., M.L., D.P., F.B., O.S., C.F., and V.H. designed research; F.G., M.J., A.P., G.K., D.P., and F.O. performed research; F.G., M.J., A.P., M.L., F.O., F.B., A.G.N., K.F., T.M., and C.F. contributed new reagents/analytic tools; F.G., M.J., A.P., G.K., M.L., D.P., C.F., and V.H. analyzed data; and C.F. and V.H. wrote the paper.

The authors declare no conflict of interest.

This article is a PNAS Direct Submission.

[1]F.G., M.J., and A.P. contributed equally to this work.

[2]To whom correspondence may be addressed. Email: christian.freund@fu-berlin.de or haucke@fmp-berlin.de.

This article contains supporting information online at www.pnas.org/lookup/suppl/doi:10.1073/pnas.1715341114/-/DCSupplemental.

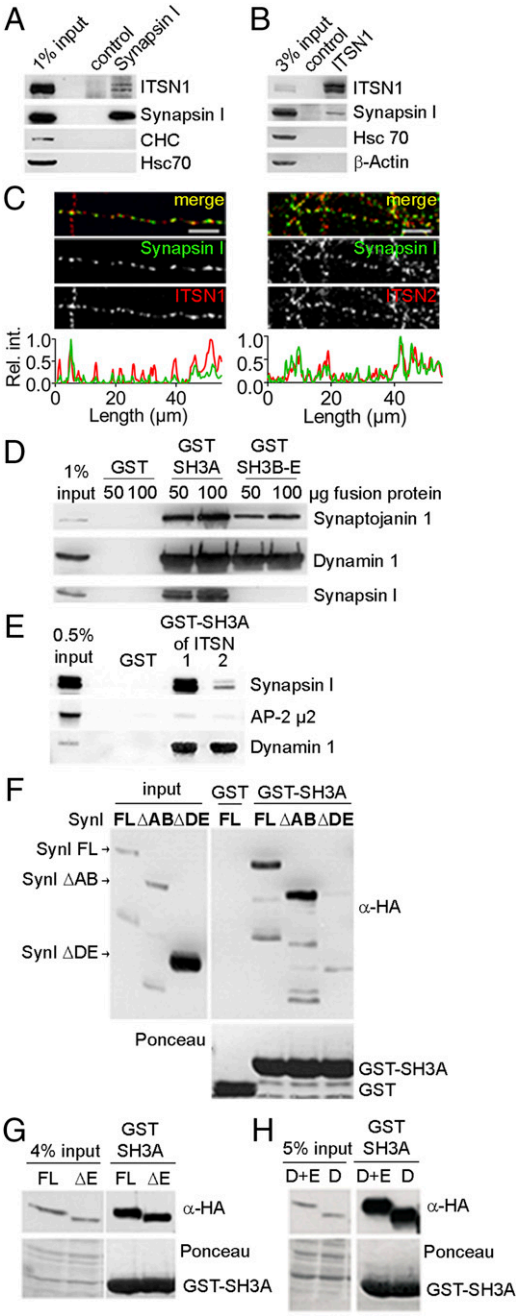

Fig. 1. Intersectin 1/2 associate with synapsin I. (*A* and *B*) Synapsin I and intersectin 1 form a complex. Immunoprecipitation from detergent-extracted rat brain lysates using specific antibodies. Samples were analyzed by immunoblotting. CHC, clathrin heavy chain; Hsc70, heat shock cognate protein 70; ITSN1, intersectin 1. (*C*) Intersectin 1 and 2 colocalize with synapsin I at hippocampal synapses. (*Upper*) Hippocampal neurons were immunostained with antibodies against synapsin I and intersectin 1 (*Left*) or 2 (*Right*). (*Lower*) Intensity line scans of representative axon segments show immunofluorescent spikes of synapsin 1 (green trace) and intersectin 1 or 2 (red trace). (Scale bars: 10 μm.) (*D*) Synapsin binds intersectin 1-SH3A. Immunoblots of pulldowns from rat brain extracts with immobilized GST fusion proteins. (*E*) As in *D* using GST-SH3A domains of intersectin 1 or 2 or GST as a control. (*F–H*) The intersectin 1-SH3A domain binds to the synapsin D domain. Shown are anti-HA immunoblots of pulldowns from detergent-extracted Cos7 cell lysates expressing the indicated synapsin Ia mutants. See Fig. S1*B*.

machinery. Mass spectrometry analysis and immunoblotting of native immunoprecipitates from brain lysates captured by antibodies (Tables S1 and S2) against the abundant presynaptic protein synapsin I identified the SH3 domain scaffold protein intersectin 1 as a synapsin-binding partner (Fig. 1*A*). Conversely, synapsin I was found in intersectin 1 immunoprecipitates (Fig. 1*B*). Moreover, synapsin I and intersectin 1 colocalized at synapses of cultured hippocampal neurons (Fig. 1*C*), consistent with the enrichment of both proteins within the presynaptic compartment at the ultrastructural level (20). Hence, intersectin and synapsin I are present in a complex at mammalian synapses in vivo, in agreement with the ability of synapsins to bind to SH3 domain-containing proteins (21).

Mammalian intersectin 1 contains five sequential SH3 domains (SH3A–E) (14) that enable interactions with proline-rich regions of exo/endocytic proteins. To assess if these SH3 domains mediate the formation of a complex with synapsin I, affinity purification experiments employing GST fusion proteins were performed. Synapsin I avidly bound to the isolated SH3A domain of intersectin 1, but not to an SH3B–E domain array (Fig. 1*D*). By contrast, the SH3 domain-binding endocytic proteins dynamin 1 and synaptojanin 1 interacted with either fusion protein (Fig. 1*D*). The SH3A domain of the closely related intersectin 2 also bound to synapsin I, albeit with reduced efficiency compared with intersectin 1 (Fig. 1*E*), in agreement with the partial colocalization of synapsin I with intersectin 1 and 2 at hippocampal synapses (Fig. 1*C*).

To identify the intersectin-binding determinants within synapsin I, we analyzed various truncation mutants of synapsin Ia for their ability to associate with intersectin 1-SH3A. Synapsin Ia is composed of five sequential domains, A–E (Fig. S1*B*) (6). Initial analysis of truncation mutants mapped the intersectin 1 binding to the distal D and E domains of synapsin Ia (Fig. 1*F* and Fig. S1*B*). Further truncation analysis revealed that domain E was dispensable (Fig. 1*G* and Fig. S1*B*), whereas the D domain was necessary and sufficient for the association of synapsin I with intersectin 1 (Fig. 1*H* and Fig. S1*B*).

SH3 domains are known to associate with proline-rich sequences, often flanked by basic residues. To elucidate the minimal sequence required for the interaction with intersectin 1, we searched the D domain for basic PxxP peptide (proline-rich peptide, PRP) motifs. We identified three such motifs in the D domain of synapsin Ia (Fig. S1*B*). Deletion of PRP2 in synapsin Ia significantly reduced intersectin 1 association, while simultaneous deletion of both PRP2 and PRP3 [full-length (FL) Δ*r*PRP2+3] abolished the interaction completely (Fig. S1*B*). Conversely, NMR spectroscopy confirmed the ability of PRS2 to directly bind to intersectin 1-SH3A (Fig. S1*C*).

We conclude that intersectin and synapsin associate via the recognition of proline-rich motifs within synapsin Ia that bind to the SH3A domain of intersectin 1.

Intersectin Regulates the Nanoscale Localization of Synapsin to Promote SV Replenishment. Based on the physical association of intersectin with synapsin I, we hypothesized that intersectin regulates synapsin function in vivo. To test this hypothesis, we generated intersectin 2-KO (hereafter "2KO") mice (Fig. S2*A*) and crossed them with intersectin 1-KO (hereafter, "1KO") mice (16) to obtain double-KO (DKO) mice lacking intersectins 1 and 2 (Fig. S2*B*). While 1KO or 2KO mice showed a Mendelian distribution and were viable and fertile, DKO mice were born well below Mendelian ratios (Fig. 2*A*), and the surviving animals suffered from decreased postnatal viability (Fig. 2*B*) and displayed reduced weight (Fig. 2*C*), in contrast to an earlier study using a Gene Trap-based intersectin 1 line (22). A significant weight reduction was already observed in compound KO mice lacking the two intersectin 1 alleles and one intersectin 2 allele (Fig. 2*C*). Furthermore, DKO mice displayed behavioral abnormalities such as strongly reduced digging (Fig. S2*C*), a phenotype related to autism spectrum disorders and also observed in synapsin-KO mice (11).

Loss of intersectins 1/2 did not affect the expression or presynaptic levels of SV proteins, including synapsin I, or any other exo/endocytic protein analyzed (Figs. S2*D* and S3*A*). Consistent with the normal SV protein levels, analysis by electron microscopy did not reveal overt differences in the total SV density or in the number of docked SVs at steady state (Fig. S3*B*). Although not

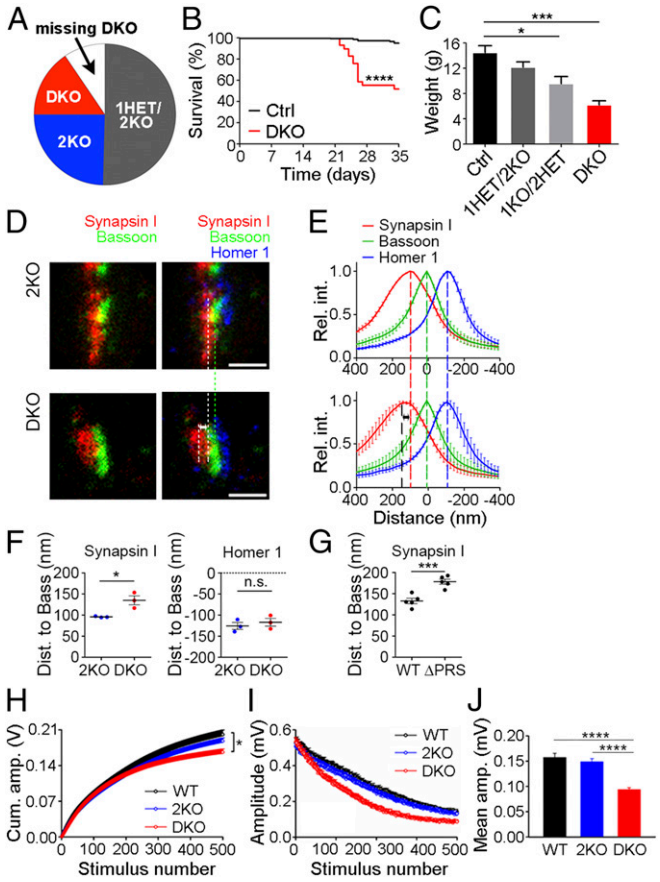

Fig. 2. Intersectin 1/2 regulates synapsin I nanoscale distribution and presynaptic function. (*A*) Genotype distribution in 249 litters of intersectin 1HET/2KO mice. Thirty-eight percent fewer DKO mice were born than would be expected from a Mendelian distribution. (*B*) Kaplan–Meier survival analysis of DKO ($n = 29$) and control animals (all other allelic combinations; $n = 144$). Statistical analysis by log-rank (Mantel–Cox) test and Gehan–Breslow–Wilcoxon test. (*C*) Weight of male DKO mice and controls (postnatal day 21–36). DKO mice show a dramatically reduced weight with the lightest mice being the most prone to die ($n_{(\text{controls = other genotypes})} = 33$; $n_{(\text{intersectin 1HET/2KO})} = 18$; $n_{(\text{intersectin 1KO/2HET})} = 9$; $n_{(\text{DKO})} = 8$); one-way ANOVA followed by Tukey's posttest. (*D–F*) Altered nanoscale localization of synapsin I in DKO hippocampal neurons. Neurons were immunolabeled with antibodies against synapsin I, bassoon, and homer 1 and were imaged by three-channel time-gated STED (gSTED). (*D*) Representative sum intensity projected gSTED images displayed as two- or three-channel overlays show an increased distance between synapsin I and bassoon in DKO synapses. (Scale bars: 500 nm.) (*E*) Averaged aligned line profiles from 314–343 synapses show an increased distance between synapsin I and bassoon (set to 0 nm) in DKO synapses. Colored dashed lines indicate maximum values of intersectin 2KO used as control. The black dashed line indicates the maximum value for synapsin in DKO synapses. Data are expressed as mean ± SEM. (*F*) Average distances between synapsin I and homer 1 and bassoon. Data are from three independent experiments with 40–171 synapses each; unpaired Student's *t* test, $^*P < 0.05$; n.s., not significant. (*G*) Average distance of WT or ΔPRS mutant synapsin IA–E–GFP from bassoon. Data are from five independent experiments; paired Student's *t* test; $^{***}P = 0.0008$. (*H–J*) Reduced cumulative response amplitudes in acute slices from DKO mice stimulated with 500 stimuli at 20 Hz. (*H*) Cumulative amplitudes were significantly different between genotypes by one-way RM ANOVA ($P = 0.01$), and the HS test showed a significant difference between WT and DKO mice ($P = 0.02$) at the 500th pulse. (*I*) Accelerated synaptic rundown during stimulation with 500 pulses in DKO slices. (*J*) Results extracted from *I* show reduced mean amplitudes of responses between stimulus pulses 400 and 500. One-way RM ANOVA ($P < 0.0001$), followed by the HS test indicates significant differences between WT and DKO ($P < 0.0001$) as well as between 2KO and DKO ($P < 0.0001$; WT, $n = 12$, $N = 4$; 2KO, $n = 14$, $N = 6$; DKO, $n = 11$, $N = 5$). All column diagrams display mean ± SEM.

required for synapsin I expression, it is conceivable that intersectin may regulate the localization of synapsin within the presynaptic compartment. To address this question we first studied the effect of intersectin 1/2 loss on the activity-induced axonal dispersion and reclustering of synapsin I (23). We observed similar activity-induced dispersion of synapsin I into the axon, followed by its reclustering into presynaptic puncta reflecting reassociation with reserve pool SVs (6, 23) in hippocampal neurons from intersectin 1/2 DKO mice and from phenotypically normal 2KO littermates used as control (Fig. S3*C*). Thus, intersectin is not required for synapsin association with or dissociation from SVs.

Next we analyzed the effect of intersectin 1/2 loss on the nanoscale distribution of synapsin I by isotropic multicolor time-gated stimulated emission depletion microscopy (time-gated STED) (Fig. S4 *A* and *B*). To this aim, hippocampal neurons were triply stained for synapsin I, the AZ marker bassoon, and the postsynaptic scaffold homer 1. Acquired z-stacks were summed, and the distribution of each marker along line profiles perpendicular to bassoon and homer 1 labeling were quantitatively analyzed (Fig. S4*B*). The AZ marker bassoon was located at a mean distance of about 120 nm from postsynaptic homer 1^+ sites, consistent with recent stochastic optical reconstruction microscopy (STORM) microscopy data (24), and this distribution was unaffected by the absence of intersectin 1/2 (2KO: 125 nm ± 8.2 nm; DKO: 117 ± 9.1 nm) (Fig. 2 *D–F*). In contrast, we found a marked shift of the synapsin I peak away from the AZ center in intersectin 1/2-DKO neurons (2KO: 95 nm ± 0.9 nm; DKO: 135 nm ± 10 nm) (Fig. 2 *D–F*). A similar shift was seen when the distribution of intersectin-binding–defective mutant synapsin I (FLΔPRP2+3) (Fig. S1*B*) expressed in WT neurons was analyzed (synapsin$I^{\Delta PRS}$) (Fig. 2*G* and Fig. S4 *I* and *J*). Loss of intersectin 1/2 did not affect the nanoscale distribution of endophilin A1 or the clathrin adaptor AP2, endocytic proteins associated with intersectin (Fig. S4 *C–H*). These data show that intersectin regulates the nanoscale distribution of synapsin I at central mammalian synapses, in agreement with the physical association of the two proteins.

Previous data had shown that the synapsin-dependent reserve SV pool mediates the replenishment of the recycling vesicle pool (5) during periods of sustained activity (7, 25). We therefore analyzed synaptic transmission in acute slice preparations from intersectin single-KO or DKO mice. Single or combined loss of intersectins 1 and 2 had no effect on baseline synaptic transmission measured as fiber volley (FV) and field excitatory postsynaptic potential (fEPSP) amplitude ratios over a range of stimulation intensities (Fig. S5 *A* and *B*). However, when challenged by sustained stimulation with 500 pulses at 20 Hz [an established protocol to probe vesicle replenishment (26)], intersectin 1/2-deficient synapses showed a significant reduction in their cumulative amplitudes compared with WT controls (Fig. 2*H*), while the initial AMPA receptor (AMPAR)-mediated responses were similar (Fig. S5*C*). This deficit was caused by enhanced synaptic rundown following 150 or more stimulation pulses (Fig. 2*H*) due to a reduced rate of SV replenishment in the absence of intersectin 1/2 (Fig. 2 *I* and *J*). A similar activity-dependent depression of neurotransmission has been reported for synapsin I-KO mice (25, 26). The presence of one intersectin isoform was sufficient for functionality, as deletion of intersectin 1 alone did not result in defective SV replenishment (Fig. S5 *D–F*). Our data suggest that intersectin controls SV replenishment from the reserve pool at mammalian synapses, likely by regulating synapsin localization.

Formation of the Synapsin I–Intersectin 1 Complex Is Controlled by an Intramolecular Switch in Intersectin 1. Our data unravel an unexpected function of intersectin 1 in synapsin-dependent SV replenishment, in addition to its established role in endocytosis. This poses the question: Which mechanisms differentially regulate the formation of the intersectin 1–synapsin I complex at synapses? Many synaptic proteins undergo activity-regulated cycles of phosphorylation/dephosphorylation (6, 27), which often affect their formation of complexes with other proteins. We therefore analyzed

the potential role of protein phosphorylation in regulating intersectin 1–synapsin I association. Immunoprecipitations from rat brain extracts under either phosphorylation- or dephosphorylation-promoting conditions showed that the complex between intersectin 1 and synapsin I remained at the detection limit under dephosphorylating conditions but was strongly increased under phosphorylation-promoting conditions, while binding of the endocytic protein dynamin 1 was concomitantly reduced (Fig. 3 *A* and *B*). As synapsin I is one of the major brain phosphoproteins (6), we explored a potential role of synapsin I phosphorylation in regulating its association with intersectin 1. However, neither phosphorylation by protein kinase A (PKA) nor by Ca^{2+}-calmodulin–dependent protein kinase II (CaMKII) had any effect on its ability to bind intersectin (Fig. 3*C*). Alternatively, formation of the intersectin 1–synapsin complex might be regulated by phosphorylation-induced conformational changes within intersectin 1, which is heavily phosphorylated at multiple sites (https://www.phosphosite.org/homeAction.action). To further explore this possibility and delineate the intersectin 1 site responsible for such regulation, we analyzed the ability of intersectin 1-SH3 domain fragments of various lengths to bind synapsin Ia. We found that, while the isolated SH3A domain efficiently captured synapsin Ia from brain lysates, a larger protein fragment encompassing the entire SH3 domain module (SH3A–E) bound synapsin I with strikingly reduced efficiency (Fig. 3*D*), suggesting that intersectin 1 may be autoinhibited.

To gain mechanistic insights into such potential intramolecular regulation of intersectin 1, we utilized NMR spectroscopy. We used sortase-mediated ligation (Fig. S6*A*) to generate an SH3A–E construct in which the SH3A domain was selectively labeled with ^{15}N. A comparison of the spectra of the isolated ^{15}*N*-SH3A domain and the ligated ^{15}*N*-SH3A–E module revealed large chemical shift changes (Fig. 3*E* and Fig. S6*B*). These changes were similar to but larger than those observed when a fourfold excess of SH3B-E was added *in trans*, indicative of an intramolecular interaction (Fig. 3*E*). Mapping the intramolecular binding epitope onto a homology-modeled structure of the intersectin 1-SH3A domain identified a large interaction surface that includes the canonical binding site for proline-rich ligands (Fig. 3*F*). Further truncation experiments paired with affinity chromatography from brain lysates and NMR spectroscopy of ^{15}*N*-SH3A variants showed that an extension of the SH3A domain by about 20 amino acids into the linker between the SH3A and SH3B domains is sufficient to prevent synapsin I binding (Fig. S6*C*) and elicits spectral shifts similar to those seen for the ligated SH3A–E module (Fig. S6*D*). However, this 20-residue peptide does not harbor any classical class I/II SH3-binding motif (RxxPxxP or PxxPxR) (Fig. S7*A*). Subsequent peptide SPOT analysis using single alanine substitutions identified the motif PKLALR as a central determinant for SH3A binding (Fig. 3*G*). This sequence deviates from the preferred proline-rich recognition sequence of the intersectin 1-SH3A domain (PxϕPXR) determined by phage display technology (Fig. S7*B*). A suboptimal ligand may, in fact, be a prerequisite for the conformational transition that allows the intramolecular binding to be replaced by intermolecular interactions.

A prediction of this conformational switch model for intersectin function in SV cycling vs. synapsin-mediated SV replenishment is that synapsin binding should be particularly sensitive to the conformational state of the SH3A domain of intersectin 1. In contrast to dynamin, synapsin I is therefore predicted to selectively associate with the open, but not the locked, form of the domain. To test this, we used quantitative mass spectrometric analysis of labeled native protein samples to identify proteins associated with the conformationally "open" SH3A or an extended intramolecularly locked version of SH3A ("locked SH3A") when immobilized on beads (Fig. 4*A*). We identified peptides from 11 proteins as potentially specific binding partners of SH3A, which included known intersectin 1 interactors such as dynamins 1–3, synaptojanins 1/2 (14), and synapsins as well as other interactors, most notably the AZ protein piccolo (Fig. S7*C* and Table S3). Strikingly, synapsin I/II were the only proteins from these 11 candidates that associated predominantly with

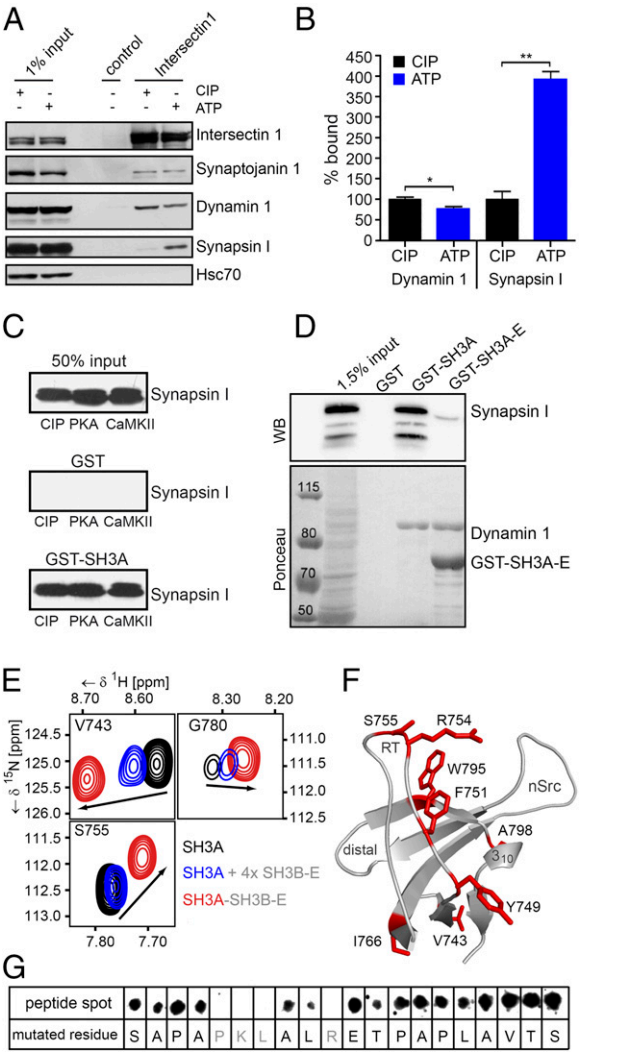

Fig. 3. Regulation of intersectin 1-SH3A domain function by an intramolecular switch. (*A* and *B*) Synapsin I preferentially binds phosphorylated intersectin 1. (*A*) Immunoprecipitations under phosphorylation-promoting (ATP) or dephosphorylation-promoting (calf intestinal phosphatase, CIP) conditions from detergent-extracted rat brain lysates. Samples were analyzed by immunoblotting. (*B*) Quantification of data shown in *A*. Data are shown as mean ± SEM; $n = 3$; $*P < 0.05$; $**P < 0.01$; Student's *t* test. (*C*) Phosphorylation of synapsin I at S9 (site 1; PKA) or at S566/S603 (sites 2/3; CaMKII) does not affect its binding to GST–intersectin 1-SH3A. Immobilized GST–intersectin 1-SH3A was incubated with in vitro dephosphorylated or phosphorylated synapsin I. Samples were analyzed by immunoblotting. Data are shown as mean ± SEM; all nonsignificant; one-way ANOVA. (*D*) Synapsin I does not interact with intersectin 1-SH3A in the context of the other SH3 domains. Immunoblot analysis of immobilized intersectin 1 GST–SH3A and GST–SH3A–E fusion proteins incubated with rat brain extract. (*E*) Intramolecular clamping of SH3A. Selected regions from overlays of ^{15}*N*-HSQC spectra of intersectin 1-SH3A recorded before (black) and after (red) ligation to SH3B-E or of SH3A after *in trans* addition of a 4× excess of SH3B-E (blue). (*F*) Epitope mapping of the SH3A intramolecular interaction. Red, residues that show chemical shift changes greater than mean ± SEM (0.11 ppm) or disappearing due to line broadening upon ligation to SH3B-E. The domain structure was predicted using the phyre2 web server (34). (*G*) Immobilized peptide spots of an 821- to 840-aa SH3A-B interdomain linker peptide with residues successively mutated to A (alanine scanning). Peptides were probed for interaction with GST-SH3A by immunoblotting. Gray, residues that lead to signal loss upon mutation.

the conformationally open but not the locked version of SH3A (Fig. 4*A* and Table S3). This confirms that the formation of the synapsin–intersectin 1 complex is regulated by the intramolecular interaction of its SH3A domain with the adjacent

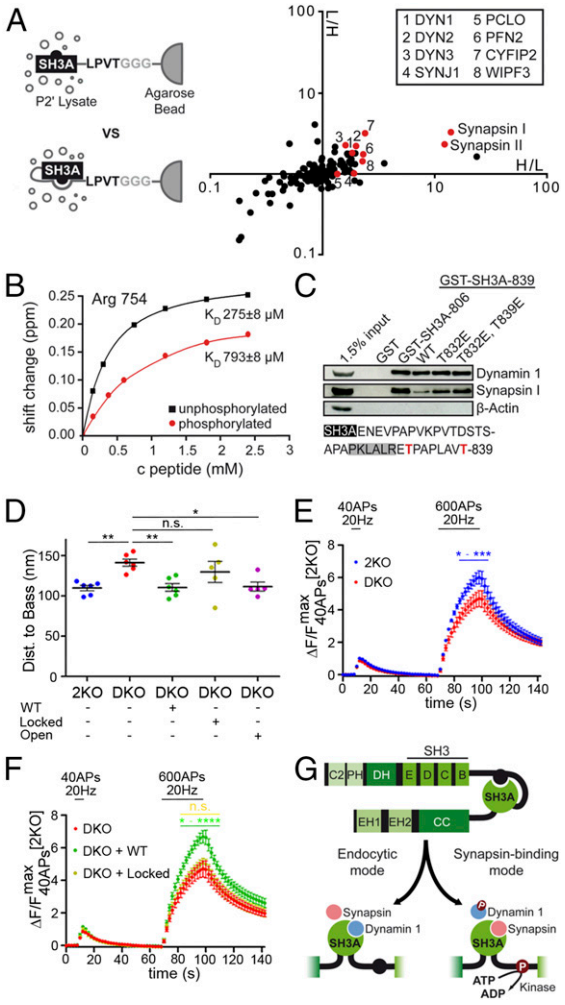

Fig. 4. The intersectin switch regulates complex formation with synapsin I. (*A*–*C*) Synapsin binds preferentially to open intersectin 1-SH3A. (*A*, *Left*) Scheme of the pull-down MS experiment. (*Right*) Scatter plot of $^{16}O/^{18}O$ isotope ratios of identified proteins (red, see Fig. S7*B* and Table S3) from two independent experiments (forward and reverse labeling). Only synapsins I/II associate preferentially with SH3A vs. locked SH3A. (*B*) NMR titration experiment (exemplary curve from signal of SH3A-R754), with an SH3A–B interdomain linker-derived peptide. Black: dephosphorylated; red: T832 and T839 phosphorylated. K_d (dephosphorylated) = 275 ± 8 µM; K_d (phosphorylated) = 793 ± 52 µM. (*C*, *Upper*) Immunoblots of pulldowns using intersectin 1 GST–SH3A with various linker lengths and mutations within the intramolecular binding site. (*Lower*) Scheme of mutated T residues (red) relative to the intramolecular binding site (gray). (*D*) WT or constitutively active open (T832E, T839E) but not locked (A828P, T832A, T839A) mutant intersectin 1 rescue-defective synapsin 1 nanoscale distribution (average distances of synapsin I to bassoon) in DKO neurons. Data are from six independent experiments; one-way ANOVA with Dunnett's posttest, $*P < 0.05$. (*E* and *F*) Average traces of synaptophysin–pHluorin–expressing neurons stimulated (20 Hz) with 40 APs (RRP; see Fig. S8 *G* and *H*) or 600 APs to measure the size of the recycling SV pool. Data were normalized to the maximum of the 40-AP peak of 2KO controls. Data are the mean ± SEM of 4–10 independent experiments; two-way RM ANOVA using Bonferroni's multiple comparisons test (control: DKO), $*P < 0.05$, $**P < 0.01$. (*E*) DKO neurons show a decreased recycling SV pool size; $*P < 0.05$, $***P < 0.001$. (*F*) WT but not locked mutant (A828P, T832A, T839A) intersectin 1 rescues the reduced recycling SV pool size in DKO neurons; $*P < 0.05$, $****P < 0.0001$. (*G*) Model for phosphoregulated conformational switching of intersectin 1 function in SV endocytosis and SV mobilization via synapsin binding.

PKLALR-containing linker sequence. Consistent with this model, NMR experiments using the selectively labeled SH3A–E construct showed that a 10-fold molar excess of a dynamin-based PRP was able to compete and thus open the intramolecular lock on SH3A, while the synapsin-derived PRP2 peptide did not (Fig. S7*D*).

These results further suggest that phosphorylation could be necessary to release the clamped conformation of intersectin 1-SH3A and enable its association with synapsin to regulate SV mobilization. In line with this, two of the phosphorylation sites within intersectin 1, T832 (28) and T839 (https://www.phosphosite.org/homeAction.action), are in close proximity to the PKLALR-containing linker sequence (Fig. S7*A*). To analyze the role of these phosphosites in regulating the formation of the intersectin 1–synapsin I complex, we synthesized phosphopeptides corresponding to the PKLALR-containing linker sequence of intersectin 1 and analyzed their ability to bind to SH3A. Phosphorylation of T832/T839 caused a threefold drop in the affinity for SH3A (Fig. 4*B*), suggesting that phosphorylation of these residues substantially shifts the equilibrium toward conformational opening of intersectin 1, thereby enabling the association of synapsin I with the intersectin-SH3A domain. We tested this directly by generating phosphomimetic mutants of the extended SH3A construct. While the T832E mutation alone led to only slightly increased synapsin I binding of the corresponding GST–SH3A-linker fusion proteins, the simultaneous introduction of two phosphomimetic mutations, T832E and/or T839E, restored synapsin I binding almost to the level of constitutively open SH3A lacking the linker sequence (Fig. 4*C*).

To probe the physiological relevance of the formation of the phosphoregulated intersectin 1–synapsin I complex, we generated a nonphosphorylatable and reinforced locked mutant of intersectin 1 (A828P, T832A, T839A) unable to associate with synapsin (Fig. S7*E*) and analyzed its ability to restore the defective nanoscale distribution of synapsin I in intersectin 1/2-DKO neurons. Reexpression of WT or constitutively open intersectin 1 (T832E, T839E) in intersectin 1/2-DKO neurons shifted the nanoscale localization of synapsin I to that observed in WT neurons, while reexpression of locked mutant intersectin 1 did not (Fig. S8 *A*–*F*). To test whether complex formation with synapsin underlies the observed regulation of SV replenishment by intersectin 1/2, we measured the effects of manipulating intersectin function in hippocampal neurons using synaptophysin-pHluorin assays to probe SV pool sizes (5, 29). As expected from our electrophysiological analysis (Fig. 2), we observed that the recycling SV pool size probed by 600 action potentials (APs) applied at 20 Hz was reduced in intersectin 1/2-DKO neurons (Fig. 4 *E* and *F*). The size of the readily releasable vesicle pool (RRP) and the kinetics of exocytic release were unaltered (Fig. S8 *G* and *H*). The reduced size of the recycling SV pool was fully restored by reexpression of WT intersectin 1 in DKO neurons, whereas synapsin-binding–defective locked mutant intersectin 1 was without effect (Fig. 4 *E* and *F*).

These collective data suggest that phosphorylation triggers a conformational opening of intersectin 1 to allow its SH3A domain to form a complex with synapsin I (Fig. 4*G*) and thereby regulate mobilization of reserve pool SVs.

Discussion

We show here by superresolution microscopy and by complementary genetic, electrophysiological, and biochemical approaches that intersectin 1 regulates SV replenishment through interactions with synapsin I. The defective nanoscale localization of synapsin I in synapses from intersectin 1/2-DKO mice correlates with and likely underlies impaired replenishment of SVs from the synapsin-dependent reserve pool under conditions of sustained stimulation, while the RRP and the overall number of SVs are unaltered. Impaired sustained neurotransmission is a hallmark of synapsin-KO mice (6, 25), which suffer from a greatly reduced recycling SV pool due to SV dispersion into the axon. We propose a model based on these data in which intersectin 1/2, in addition to its proposed role in SV endocytosis and/or recycling (14), fulfills a second presynaptic function in regulating SV replenishment from the reserve pool (5) via its association with synapsin I.

During sustained stimulation the activity-dependent phosphorylation of synapsin reduces its affinity for SV membranes to

allow SV mobilization for the replenishment of the recycling SV pool (6). Although the precise mechanism of intersectin action in SV replenishment remains to be determined, one possibility supported by our superresolution imaging data is that intersectin, a protein absent from SVs (30), acts as a molecular sink within the periactive zone that locally sequesters free synapsin I under conditions of sustained activity. This prevents premature rebinding of synapsin I to SVs and thereby resequestering SVs into the reserve pool, and thus facilitates the refilling of the RRP that drives exocytosis.

An important finding from our study is that the affinity of the intramolecular interaction in intersectin is finely tuned for its low-affinity interaction partner synapsin I and that phosphorylation at multiple sites, including T832 and T839, controls access to its SH3A domain. The precise signaling pathways that control intersectin phosphorylation remain to be determined. Presynaptic neurotransmission is regulated by several protein kinases, most notably cyclin-dependent kinase 5 (Cdk5) (31) but also others such as CaMK or PKA (6) that may conceivably phosphorylate intersectin 1 to enable SV replenishment under conditions of sustained activity. In addition to these phosphoregulatory mechanisms, the synapsin I–intersectin 1 complex may be regulated by other intersectin-binding partners. Irrespective of these mechanistic considerations, our data unravel a molecular link between the synapsin-dependent reserve SV pool and the presynaptic endocytosis machinery. Furthermore, the physical and functional association of intersectins (22) and synapsins may underlie the role of these proteins in learning and memory and in the pathogenesis of neurological disorders (32, 33).

Materials and Methods

All experiments in the present study were conducted in accordance with the guidelines of the Landesamt für Gesundheit und Soziales Berlin (LAGeSo) and with their permission. Intersectin 1/2-DKO mice were bred under the license G0357/13 by the LAGeSo.

Acquisition of ^{1}H-^{15}N Heteronuclear Single-Quantum Correlation Spectra. 2D heteronuclear single-quantum correlation (HSQC) spectra were recorded on a Bruker UltraShield 700 Plus equipped with a 5-mm triple-resonance cryoprobe. Measurement of the ^{15}N-labeled intersectin 1 domain, as well as selectively labeled five-domain constructs, was accomplished at 298 K and protein concentrations of 100–200 μM (isolated domains) or 40–60 μM (ligated five-domain constructs). Samples with a volume of 550–660 μL were buffered in a modified PBS (50 mM NaCl, 2.7 mM KCl, 10 mM Na_2HPO_4, 2 mM KH_2PO_4, 0.5 mM EDTA, pH 7.5) + 10% (vol/vol) D_2O. Complex data points (1,024 × 128) were acquired with eight (isolated domains) or 40 (ligated five-domain constructs) scans in each HSQC experiment. Resulting spectra were processed using TopSpin 3.2 (Bruker), and figures were prepared using Sparky 3.1.1.1 (T. D. Goddard and D. G. Kneller, University of California, San Francisco).

Statistical Analysis. Quantifications for biochemical experiments were always based on at least three independent experiments. Statistical data evaluation was performed using GraphPad Prism 4 software. Student's *t* tests and one-way ANOVA tests with Tukey's posttest were used to compare means if not stated otherwise in the figure legends. Electrophysiological data were statistically evaluated with SigmaStat using Student's *t* tests or repeated-measures (RM) ANOVA with the factor genotype. Significant differences were accepted at $****P < 0.0001$; $*P < 0.05$. When several genotypes were compared, ANOVA tests were followed by a Holm–Sidak (HS) posttest to detect differences between experimental groups. *N* indicates the number of animals or cell cultures used; *n* indicates the numbers of slices measured or the number of synapses analyzed in the data shown in Figs. 2 and 4 and Figs. S5 and S8.

For further information, see *SI Materials and Methods* available online.

ACKNOWLEDGMENTS. We thank Claudia Schmidt, Maria Mühlbauer, Delia Löwe, and Silke Zillmann for expert technical assistance. This work was supported by German Research Foundation Grants SFB958/A07 and -/Z03 (to C.F. and V.H.) and SFB958/A01 (to T.M. and V.H.), NeuroCure Cluster of Excellence Grant Exc-257 (to V.H.), and Telethon-Italy Grant GGP13033, CARIPLO Grant 2013-0879, and Italian Ministry of Health Grant RF 2013 (to F.B.).

1. Haucke V, Neher E, Sigrist SJ (2011) Protein scaffolds in the coupling of synaptic exocytosis and endocytosis. *Nat Rev Neurosci* 12:127–138.
2. Sudhof TC (2004) The synaptic vesicle cycle. *Annu Rev Neurosci* 27:509–547.
3. Kononenko NL, Haucke V (2015) Molecular mechanisms of presynaptic membrane retrieval and synaptic vesicle reformation. *Neuron* 85:484–496.
4. Saheki Y, De Camilli P (2012) Synaptic vesicle endocytosis. *Cold Spring Harb Perspect Biol* 4:a005645.
5. Rizzoli SO, Betz WJ (2005) Synaptic vesicle pools. *Nat Rev Neurosci* 6:57–69.
6. Cesca F, Baldelli P, Valtorta F, Benfenati F (2010) The synapsins: Key actors of synapse function and plasticity. *Prog Neurobiol* 91:313–348.
7. Fornasiero EF, et al. (2012) Synapsins contribute to the dynamic spatial organization of synaptic vesicles in an activity-dependent manner. *J Neurosci* 32:12214–12227.
8. Rosahl TW, et al. (1995) Essential functions of synapsins I and II in synaptic vesicle regulation. *Nature* 375:488–493.
9. Baldelli P, Fassio A, Valtorta F, Benfenati F (2007) Lack of synapsin I reduces the readily releasable pool of synaptic vesicles at central inhibitory synapses. *J Neurosci* 27: 13520–13531.
10. Farisello P, et al. (2013) Synaptic and extrasynaptic origin of the excitation/inhibition imbalance in the hippocampus of synapsin I/II/III knockout mice. *Cereb Cortex* 23: 581–593.
11. Greco B, et al. (2013) Autism-related behavioral abnormalities in synapsin knockout mice. *Behav Brain Res* 251:65–74.
12. Fassio A, et al. (2011) SYN1 loss-of-function mutations in autism and partial epilepsy cause impaired synaptic function. *Hum Mol Genet* 20:2297–2307.
13. Denker A, Kröhnert K, Bückers J, Neher E, Rizzoli SO (2011) The reserve pool of synaptic vesicles acts as a buffer for proteins involved in synaptic vesicle recycling. *Proc Natl Acad Sci USA* 108:17183–17188.
14. Pechstein A, Shupliakov O, Haucke V (2010) Intersectin 1: A versatile actor in the synaptic vesicle cycle. *Biochem Soc Trans* 38:181–186.
15. Sakaba T, et al. (2013) Fast neurotransmitter release regulated by the endocytic scaffold intersectin. *Proc Natl Acad Sci USA* 110:8266–8271.
16. Yu Y, et al. (2008) Mice deficient for the chromosome 21 ortholog Itsn1 exhibit vesicle-trafficking abnormalities. *Hum Mol Genet* 17:3281–3290.
17. Dierssen M, et al. (2001) Functional genomics of Down syndrome: A multidisciplinary approach. *J Neural Transm Suppl* 131–148.
18. Koh TW, Verstreken P, Bellen HJ (2004) Dap160/intersectin acts as a stabilizing scaffold required for synaptic development and vesicle endocytosis. *Neuron* 43:193–205.
19. Winther AM, et al. (2015) An endocytic scaffolding protein together with synapsin regulates synaptic vesicle clustering in the Drosophila neuromuscular junction. *J Neurosci* 35:14756–14770.
20. Pechstein A, et al. (2010) Regulation of synaptic vesicle recycling by complex formation between intersectin 1 and the clathrin adaptor complex AP2. *Proc Natl Acad Sci USA* 107:4206–4211.
21. Onofri F, et al. (2000) Specificity of the binding of synapsin I to Src homology 3 domains. *J Biol Chem* 275:29857–29867.
22. Sengar AS, et al. (2013) Vertebrate intersectin1 is repurposed to facilitate cortical midline connectivity and higher order cognition. *J Neurosci* 33:4055–4065.
23. Chi P, Greengard P, Ryan TA (2001) Synapsin dispersion and reclustering during synaptic activity. *Nat Neurosci* 4:1187–1193.
24. Dani A, Huang B, Bergan J, Dulac C, Zhuang X (2010) Superresolution imaging of chemical synapses in the brain. *Neuron* 68:843–856.
25. Vasileva M, Horstmann H, Geumann C, Gitler D, Kuner T (2012) Synapsin-dependent reserve pool of synaptic vesicles supports replenishment of the readily releasable pool under intense synaptic transmission. *Eur J Neurosci* 36:3005–3020.
26. Gitler D, et al. (2004) Different presynaptic roles of synapsins at excitatory and inhibitory synapses. *J Neurosci* 24:11368–11380.
27. Cousin MA, Robinson PJ (2001) The dephosphins: Dephosphorylation by calcineurin triggers synaptic vesicle endocytosis. *Trends Neurosci* 24:659–665.
28. Giansanti P, et al. (2015) An augmented multiple-protease-based human phosphopeptide atlas. *Cell Rep* 11:1834–1843.
29. Ryan TA, Li L, Chin LS, Greengard P, Smith SJ (1996) Synaptic vesicle recycling in synapsin I knock-out mice. *J Cell Biol* 134:1219–1227.
30. Takamori S, et al. (2006) Molecular anatomy of a trafficking organelle. *Cell* 127:831–846.
31. Kim SH, Ryan TA (2010) CDK5 serves as a major control point in neurotransmitter release. *Neuron* 67:797–809.
32. Garcia CC, et al. (2004) Identification of a mutation in synapsin I, a synaptic vesicle protein, in a family with epilepsy. *J Med Genet* 41:183–186.
33. Lakhan R, Kalita J, Misra UK, Kumari R, Mittal B (2010) Association of intronic polymorphism rs3773364 A>G in synapsin-2 gene with idiopathic epilepsy. *Synapse* 64:403–408.
34. Kelley LA, Sternberg MJ (2009) Protein structure prediction on the web: A case study using the Phyre server. *Nat Protoc* 4:363–371.
35. Kuropka B, Royla N, Freund C, Krause E (2015) Sortase A mediated site-specific immobilization for identification of protein interactions in affinity purification-mass spectrometry experiments. *Proteomics* 15:1230–1234.
36. Kofler M, et al. (2009) Proline-rich sequence recognition: I. Marking GYF and WW domain assembly sites in early spliceosomal complexes. *Mol Cell Proteomics* 8:2461–2473.